Ring-Stiffness Evaluation and Optimization of Structured-Wall Polyethylene Pipes

F. Fuerle[1], J. Sienz[1], M. Innocente[1]
J.F.T. Pittman[1], V. Samaras[2] and S. Thomas[2]
[1] C[2]EC, School of Engineering
Swansea University, United Kingdom
[2] Asset International Ltd., Newport, United Kingdom

Abstract

Structured-wall high density polyethylene pipes up to 3m diameter are used extensively in civil engineering applications including storm water attenuation tanks, culverts, surface drainage, inter-process pipe work, sewers etc. The pipes are manufactured by extruding a hollow box section which is wound in a spiral manner onto a mandrel with successive turns welded together using PE from an auxiliary extruder. A key quality control measure is the ring stiffness to BS EN 1446: 1996. The ability to predict this accurately as a function of the pipe wall geometry is a pre-requisite for optimization of the pipe design. The paper describes the development and the validation of finite element modeling of the ring stiffness test in comparison with experimental results, and considers the relationship between the test results and in-situ performance. Approaches to optimizing the pipe wall structure are also outlined.

Keywords: simulation, optimization, material testing, polyethylene pipes, automatic model generation.

1 Introduction

The structured wall pipes studied within the present work are produced by winding an extruded high density polyethylene (HDPE) box profile around a mandrel and welding each turn to the adjacent one (see Figure 1).

The main objective of the current study is the development of a fast and accurate numerical simulation of the standardized ring flexibility test according to the standard BS EN 1446: 1996 (for more information the reader is referred to [1]). This standard specifies a method to measure the flexibility of a thermoplastic pipe with a circular cross section. To conduct such a test, an approximately 1-meter-wide pipe sample is placed in a compression testing machine, as shown in Figure 2.

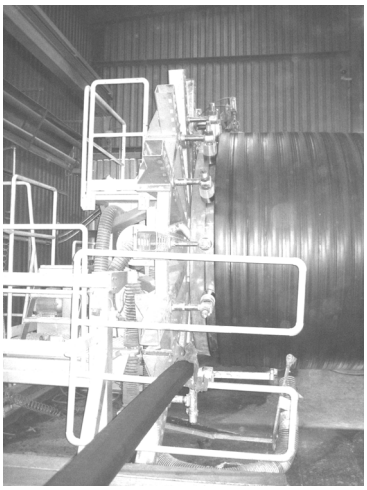

Figure 1: The profile is wound around a mandrel and welded to the adjacent one.

Figure 2: A pipe sample placed in the pipe stiffness machine.

When compressing the sample between the two parallel plates, the machine monitors the force (F) that is necessary to move one of the plates with constant velocity. According to the standard, the ring flexibility (SN) is calculated at a vertical deflection equal to 3% of the pipe's inner diameter, as shown in Equation 1, where y is the vertical deflection, L is the length of the pipe sample, and D is the inner diameter.

$$SN = \frac{F \cdot \left(0.0186 + 0.025 \cdot \frac{y}{D} \right)}{y \cdot L} \tag{1}$$

Future work will look at the improvement of the pipe's performance, as well as the minimization of the expended material. At the present stage the pipe's performance testing is restricted to that in the stiffness test. Thus the pre-requisite for the optimization of the pipe's profile is an accurate simulation of that stiffness test with low computational costs.

The present paper is structured as follows: First the material behaviour of plastics is reviewed and the conducted material tests are presented. Then the developed automated procedure for the generation of finite element (FE) models from scanned pipe profiles is discussed. Subsequently, several approaches to FE simulations are presented by looking at different element types and various possible boundary conditions. Furthermore, an application of optimization is outlined and finally the results of the work are presented.

2 Material Testing

The response of a strip of a linear elastic material subjected to a constant uniaxial stress σ_0 can be obtained with Hooke's law $\sigma_0 = E \cdot \varepsilon_0$. That means the resulting strain ε_0 is independent with respect to time. For plastics this relationship is not valid. According to [2] the material behaviour of a plastic material can be simulated by the combination of a spring, a dashpot and a Voigt element (see Figure 3). Thus

the strain occurring due to a constant stress is made up of the sum of three types of strain. The strain that is independent upon time and thus follows Hooke's law is called elastic strain ε_I. The strain that recovers sometime after unloading is called retarded elastic strain ε_{II}. The remaining part is the viscous strain ε_{III}, which will recover only in infinitely long time.

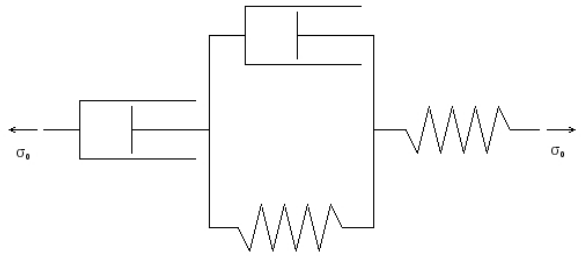

Figure 3: Model representing the behaviour of a plastic subjected to uniaxial tension – a series of a spring, a dashpot and a Voigt element.

The material behaviour certainly changes if the total stress is not immediately but gradually applied. In that case the rate at which it is increased changes the response of the material. Other factors that influence the way the material behaves are the temperature and the total stress that is applied.
The above discussion indicates that an accurate simulation of a material behaviour of that complexity, for instance within the FE method, naturally requires a nonlinear material model. Due to the high computational effort such models should be avoided in optimization processes.
Nevertheless the three factors strain, strain rate and temperature should be considered to some extent, ideally while using a linear elastic model.
If the material model is of the linear elastic type, only one representative set of material properties can be used per simulation. Therefore it has to be chosen in a way that it represents the state that material of the pipe is in as closely as possible.
With regards to the temperature, one can assume that a pipe that is stored in a location of constant ambient temperature has no variation across its volume. Therefore no error is made if material properties are known for the specific temperature. Uniformity in that sense naturally cannot be assumed for the strain field. That means both, the strain and the strain rate, cannot be respected in a satisfying way with a single set of material properties for the entire pipe. But because of the fact that inexpensive simulations are of the essence when used in optimization processes, this inaccuracy has to be accepted as long as it is within reasonable limits.
One way to reduce the error made by utilizing a linear material model is to calculate a mean strain and, with the pipe's deformation speed at hand, a mean strain rate. With those values, corresponding material properties can be obtained.
For a linear elastic material model two material properties are required. These are the E-modulus and the Poisson's ratio. As a first step the dependence upon the strain rate and the temperature of the E-modulus is going to be investigated. The Poisson's ratio will be assumed to be 0.4 and might be determined in a later stage.

In a Dynamic Mechanical Thermal Analysis (DMTA) a specimen is typically tested by applying an oscillating force or displacement, while passing through a specified temperature interval. Furthermore within one test, the oscillation frequency can take several values. This testing procedure is a convenient way to investigate the material stiffness at various temperatures, while analyzing the visco-elastic behaviour at the same time, by utilizing different frequencies.
Within the presented work, the specimens are tested in a three point bending test, where all three supports are fully clamped. A typical specimen can be seen in Figure 4.
Each of the two spans is 14 mm long, around 7 mm wide and 2.4 mm thick. Nine tests were conducted with samples from three different locations in the pipe. Each test was carried out with a temperature between -10 ºC and 90 ºC, which changed at a rate of 1 ºC/min. The middle support's maximum deformation was set to 20µm in either direction. The chosen frequencies were 10, 3, 1, 0.3 and 0.1 Hz.
From Figure 5 one can see that the theoretical moment at the supports is $6\ EI\ d/\ l^2$, where d is the displacement of one of the supports.

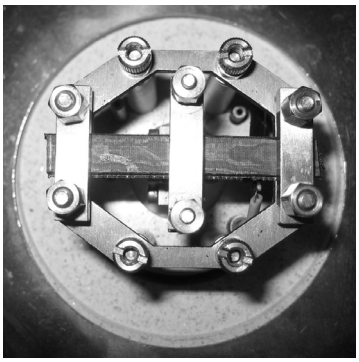

Figure 4: Specimen in clamped three point bending device of the DMTA machine. The middle support is subjected to an oscillating displacement.

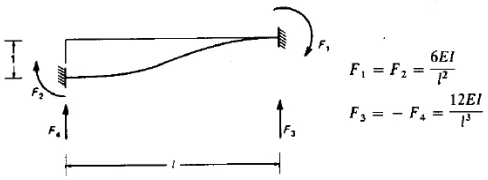

Figure 5: Theoretical moments and forces at the supports of the clamped bending test.

The bending strain is $M\ y/\ EI$, where y is the distance from the centre of gravity of the cross section to the location where the strain is desired. This desired strain is located halfway between the centre of gravity and the extreme fiber. That means that the bending strain at a support is $6\ d\ y/\ l^2$. Inserting the sample length of 14 mm, a distance between the centre of gravity and the location of the desired strain equal to 0.6 mm, as well as a deflection of 20 µm, a strain of 3.67E-04 is obtained. The strain rate is simply the strain divided by a quarter of the period. Thus the strain rate is $1.47 \cdot 10^{-3} \cdot f$, where f is the frequency of the oscillating displacement. Thus for a frequency of 0.1 s^{-1} the strain rate amounts to 1.47E-04 s^{-1}.
The resulting averaged E-moduli for various frequencies of all DMTA tests can be seen in Figure 6.
The strong dependency of the stiffness upon both the temperature and the strain rate is clearly observable. Note that especially for the lower frequencies, the results can become inaccurate towards the temperature boundaries, because the required time for one period increases and thus fewer measurements can be taken.

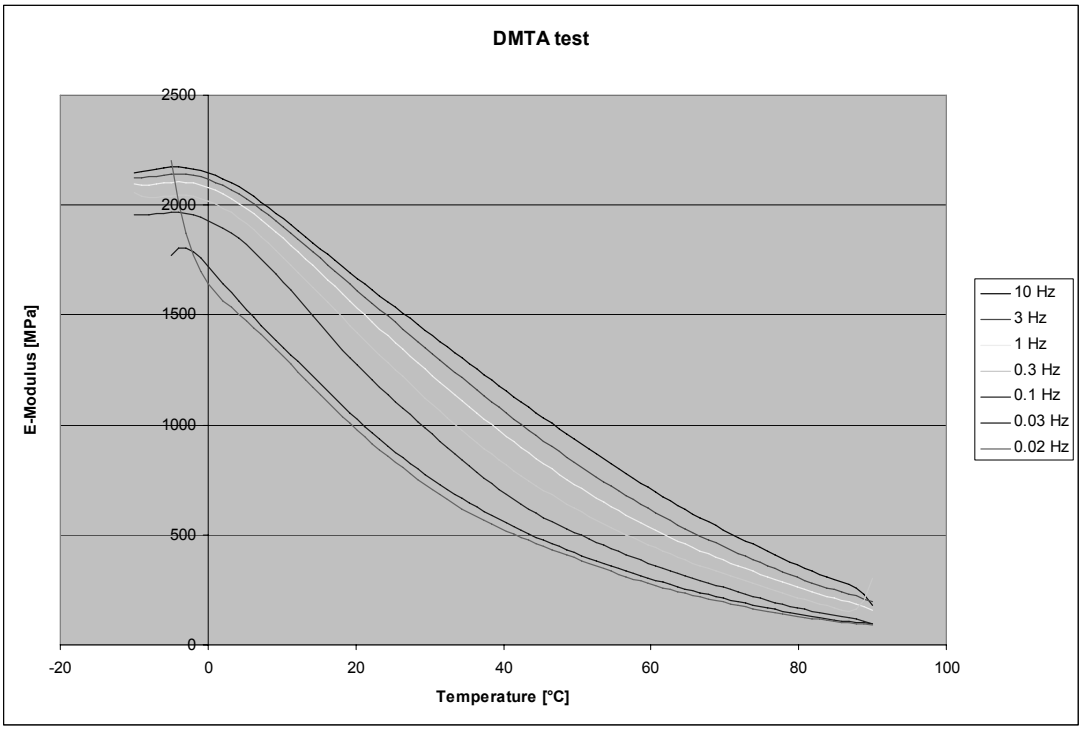

Figure 6: Temperature plotted against averaged E-modulus for various frequencies.

A representative E-modulus was found by the investigation of a pipe with a diameter of 1.5 m. The reference temperature was chosen to be 17ºC. FE analyses yielded a maximum strain intensity of around $8.0 \cdot 10^{-3}$. Taking the representative value to be half that maximum and a duration of that test of 54 seconds, the strain rate equals to 7.407E-05 s^{-1}. Temperature and strain rate interpolation then yield an E-modulus of 1200 MPa.

3 Automated Finite Element Model Generation

The theoretical, rectangular box-section profiles of the pipes, extruded at the very beginning of the production process – completely defined by the height, width and wall thicknesses – significantly differ from the cross sections obtained after production, exhibiting differences of up to 20 %. It should be noticed that the accurate measurement of the profile's height is of utmost importance, since it affects the moment of inertia with a power of three. Therefore, it was decided to cut samples of real profiles and scan their precise cross sections.

The scanning process returns files of discrete data points, distributed over the entire cross section. These points have to be processed prior to the creation of the FE model. The programs carrying out that task are written in FORTRAN 77 and the whole procedure is controlled by means of a Java tool. The latter serves as a Graphical User Interface (GUI) and simplifies the use of the command-line-type FORTRAN programs. Furthermore, it stores and manages the entered data. Java was chosen, since it provides a convenient way for the development of graphics, whereas FORTRAN was chosen for its known computational efficiency.

The scan processing starts with the rotation of the profile in a way that all walls are either horizontal or vertical. After that the repeating pattern can be identified, which is half of one box section. The identified repeating pattern and the rotated cross section are illustrated in Figure 7.

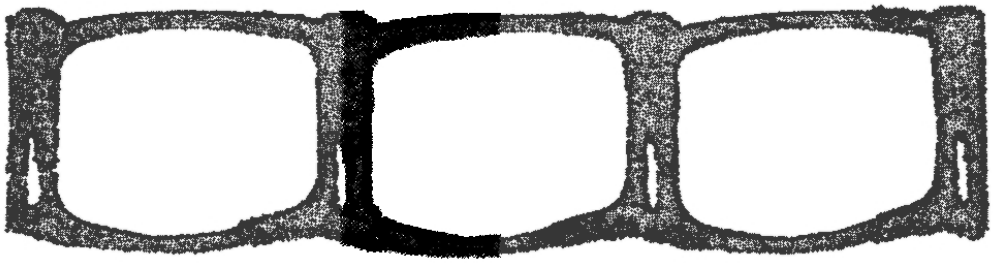

Figure 7: Rotated scanned profile with highlighted repeating pattern.

The next step is the determination which points lie on the boundary of the cross section, since only those will be of use for the model generation. After that the boundary lines have to be smoothed so that the resulting FE model does not exhibit unreal crooked edges that can cause singularities or stress concentrations. To this end, each one is replaced by a polynomial, whose parameters are found by the minimization of a least square function. That means the difference between existing discrete points and those from the polynomial is a minimum. The arising systems of equations during the determination of the coefficients of the polynomials are solved utilizing the open-source collection of mathematical subroutines LAPACK (see [2]) written in FORTRAN 77.

The generation of points that lie between the polynomial surface lines, and the definition of their corresponding thicknesses, are required next in order to generate an FE model with shell elements.

An FE model can now be created with solid elements using the polynomial approximation, or with shell elements using the points on the profile's midsurface line with the corresponding thicknesses.

In a first stage of the present work, the commercial software package Altair Hyperworks [4] is used for the remaining pre-processing, processing and post-processing. The engaged tools from Hyperworks are Hypermesh (pre-processing), Optistruct [5] (FE solver) and Hyperview (post-processing). Hypermesh incurs the conversion of the point data into geometry data, as well as the discretization of the latter.

In order to speed up and automate the entire process, Hypermesh is accessed in batch mode instead of using the GUI. The communication is realized via command files which allow for the execution of all available tasks in the program. The first command file written contains the geometry data and commands for the creation of the material, the element properties and for the mesh generation. Hypermesh is then called in batch mode, to process the command file, and to output a file containing the information of the mesh generated. Next, the user developed FORTRAN 77 program, which manages the procedure, reads this output file, applies the boundary conditions and writes another command file containing this information. Finally, Hypermesh is called again to process the latter and output the final model to be

solved by Optistruct. The above procedure is summarized in the flowchart in Figure 8.

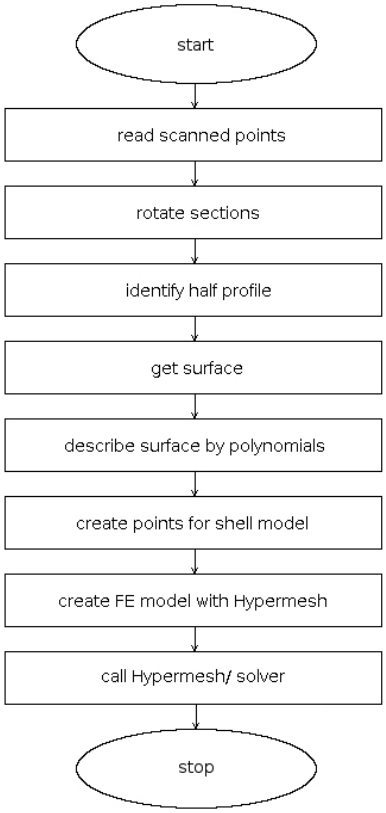

Figure 8: Flowchart of the procedure for automated FE analyses.

It is characterized by two main features. The convenience of an automated procedure, which allows for the simulation of the stiffness test of a certain pipe, is that nothing more than discrete data points of a scanned cross section and the diameter of the pipe have to be provided. At the same time the receipt of accurate geometry data is guaranteed. Summarizing one can say that a first step towards both accuracy and efficiency of the simulation has been made.
In a later stage the entire Hyperworks package has been replaced by open-source software or self-developed programs. FEAP (for further information see [6]) was substituted for Optistruct, Paraview for Hyperview and a self-developed pre-processing tool for Hypermesh.

4 Finite Element Analyses

This section discusses the different degrees of accuracy and efficiency that can be achieved in the simulation of the pipe stiffness test with the FE method. Numerous analyses are conducted in order to discuss and recommend a model with a suitable combination of accuracy and efficiency. For the simulations the material is modeled with an E-modulus of 1200 MPa and a Poisson's ratio of 0.4.

The two main aspects to be considered are the type of element and the correct boundary conditions. The analysis code used within that investigation is Optistruct. Simulations will be of the linear static type. Therefore the moving plate of the pipe stiffness experiment cannot be simulated. The constant velocity plate movement is replaced by a prescribed displacement. Furthermore, this type of simulation assumes small strain theory which is acceptable considering a pipe displacement of 3% resulting in strains of at most 0.8%.

4.1 Element Types

Two main types of element can be considered to model this problem: "solid elements" and "shell elements". The former are 3D and describe the shape of the profile more accurately, while the latter are 2½D with a certain thickness assigned. Once decided upon the use of solid or shell elements, different shapes and either linear or quadratic interpolation are also available. Finally, an adequate mesh convergence study needs to be carried out.
A solid element is commonly used for 3D structures with arbitrary shapes because the latter can be modeled with higher precision, at the cost of a higher computational effort (refer to Figure 9). Although there are numerous different types of solid elements available, only the linear (8 nodes) and quadratic (20 nodes) hexahedral elements and the linear (6 nodes) and quadratic (15 nodes) pentahedral elements were used in the current work.
A shell element is usually used for thin structures that present constant thicknesses. Since the latter is not the case for the pipe under study, the cross section is divided into smaller regions with constant thicknesses assigned. Figure 10 shows a shell model where different colors represent different thicknesses.

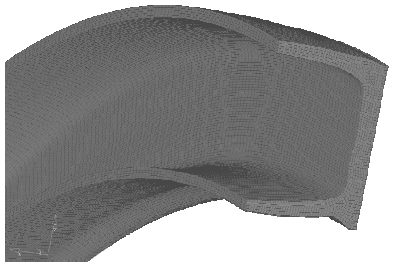

Figure 9: Solid model illustration.

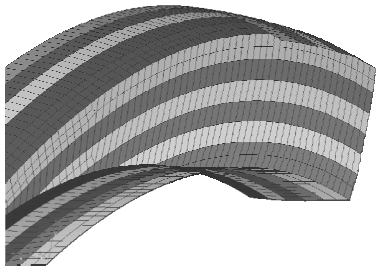

Figure 10: Shell model illustration. Different thicknesses are defined along the cross section.

On the one hand, the use of shell elements results in models with lower numbers of degrees of freedom than the use of solid elements. On the other hand, however, this introduces further simplifications to the model that might affect the accuracy of the results. While the accuracy of the global behaviour might not be jeopardized by the use of shell elements, the local behaviour certainly cannot be simulated as detailed as this is possible with solid elements. This is because the geometry cannot be represented as accurately. The shell elements considered in the current work are the

linear triangular (3 nodes) and linear quadrangular (4 nodes) elements. The corresponding quadratic elements have 6 and 8 nodes, respectively.

4.2 Boundary Conditions

The definition of the smallest model that can accurately represent the real problem directly affects the accuracy and efficiency of the simulation. In this regard, the exploitation of symmetries and definition of appropriate boundary conditions are as challenging as critical.
Clearly, both the geometry and the load state of the pipe subjected to the ring stiffness test are symmetrical with respect to all three coordinate planes. Therefore only one eighth of the whole pipe needs to be modeled, as shown in Figure 11.

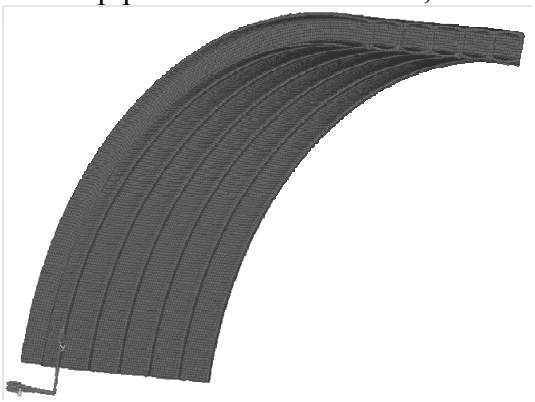

Figure 11: Real repeating pattern (one eighth of the pipe).

The boundary conditions for this model are quite straightforward: free surface on the extreme of the pipe and no displacement on the faces cut by the symmetry planes on the directions perpendicular to them or rotations about the axes contained in such planes. Finally, the displacements of the nodes in contact with the plate must be prescribed. However, in spite of the benefits of profiting from the symmetry planes, the model is still large and computationally expensive. The geometrically repeating pattern identified in Figure 7 makes it interesting to further reduce the model, although the geometrical symmetry is not extended to the boundary conditions. That is to say, the boundary conditions are not the same for every isolated geometrically repeating pattern. The latter, referred to as the "C profile" from here forth, is shown in Figure 9.
If the C-profile is to be used to model the ring stiffness test, the question is what the appropriate boundary conditions are. A color-map of the displacements in the x direction for the model with the realistic symmetry exploitation (i.e. one eighth of the pipe) is shown in Figure 12. As it can be observed, the C-profile closest to the yz symmetry plane (marked "A" in Figure 12) exhibits a behaviour that resembles the one it would have if the x-displacements of both its faces perpendicular to the x axis were restricted. On the contrary, the C-profile farthest from the yz symmetry plane (marked "B" in Figure 12) effectively has one face unrestricted, and the overall behaviour resembles the one it would have if its opposite face was perfectly restricted, except for the additional distortion due to the accumulated displacements.

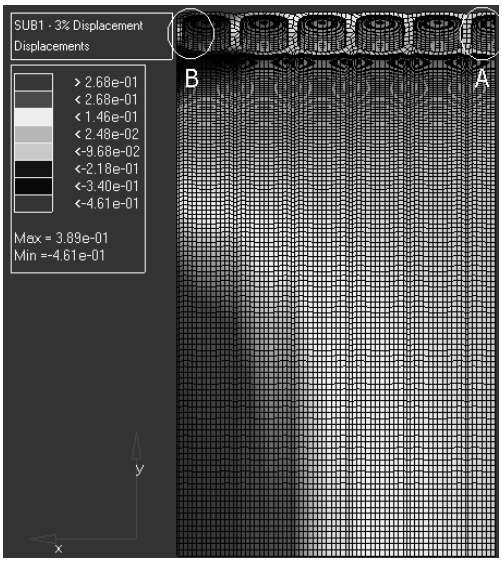

Figure 12: Component *x* of the displacements for the real repeating pattern (one eighth of the pipe).

Therefore, there is no C-profile that can realistically model the behaviour of the pipe subjected to the ring stiffness test. The best that can be aimed for is to develop some artificial boundary conditions for a C-profile – without a real counterpart – that can "represent" rather than "simulate" the real problem. That is to say, this C-profile and its boundary conditions would not be simulating any of the C-profiles in Figure 12**.** It must be kept in mind that these boundary conditions are unreal.

It seems self-evident that the ring stiffness of the pipe in Figure 11– with the real boundary conditions as described before – would be higher than that of the C-profile marked "A" in Figure 12 having the restrictive effect of the rest of the pipe simply removed (i.e. keeping its left *yz* face unrestrained). Similarly, the ring stiffness of the whole pipe would be lower than that of the same C-profile but now having the restrictive effect of the rest of the pipe replaced by a perfect restriction (i.e. forcing the *x*-displacements of its left *yz* face to zero). Hence the C-profile with the free border lower-bounds the ring stiffness of the pipe in Figure 11, while the C-profile with the restricted border upper-bounds it. However, the range of ring stiffness values bounded by these two C-models might be quite wide. Therefore, some artificial intermediate boundary condition for the left *yz* face of the C-profile "A" needs to be conceived if a C-profile is to be used to model the ring test. The great advantage of this would be that the C-model is small enough to allow numerous analyses during the optimization to be carried out in a future stage. The model that simulates one eighth of the pipe could be used to verify the results returned by the C-model.

One way to realize this desired artificial boundary condition is to use spring elements as supports at the side, where the higher or lower restrictive effect desired can be controlled by tuning the springs' stiffnesses. Thus, the latter can be adjusted in such a way that the ring stiffness obtained by using the C-profile with springs matches that of the full pipe.

It is important to keep in mind that this model cannot be used to analyze the local behaviour of specific C-profiles, but to efficiently analyze the global behaviour such as the calculation of the ring stiffness.
The spring stiffness assigned to every single spring depends upon the size of the area that every spring stands for. Thus, the concept "lateral pipe stiffness" (*lps*) is introduced in Equation 2, where S_{spring} is the spring stiffness, n_{spring} is the number of springs, A is the area that the springs are attached to, R_i and R_o are the inner and outer radii of the pipe, and h is its height of the cross section.

$$lps = \frac{S_{spring} \cdot n_{spring}}{A} \tag{2}$$

$$A = h \cdot \frac{\pi}{2} \cdot \frac{\left(R_i + R_o\right)}{2} \tag{3}$$

This concept allows that, if changes in the geometry or discretization are made, the new spring stiffness can be determined from the constant *lps* without having to tune the former until the C-model results match those of the whole model.
Since the pipe should only be stiffened in the *x*-direction, the support of each spring on the extreme that is not attached to the pipe should only be restricted in that direction. This is a kinematic configuration (i.e. not entirely constrained), which cannot be handled by linear solvers such as Optistruct. This is overcome by restraining the support in all directions, but placing it far away from the pipe so that the components on directions other than *x* are comparatively negligible.

5 Optimization

In the optimization procedure, the shell models are created by utilizing B-splines (a detailed discussion can be found in [7]). They describe the centerline, as well as the varying thickness of the cross section. To this end k key points P are generated, whose x and y coordinates, as well as thickness values are known.
The profile is then divided into three segments – two horizontal ones and one vertical one. Now the variation of the three values (coordinates and thickness) along a segment is described by means of the B-splines, which are governed by the control values b_i. The corresponding x and y component form a control point B_i. Four control points build a sub segment, which is bounded by two key points. A set of key points and the corresponding control points are depicted in Figure 13. With the control values computed, the splines can be evaluated at arbitrary locations, yielding the interpolated value for a coordinate component or the thickness.
The advantage of the above procedure, in comparison to using the key points straight away without interpolation becomes apparent, when applied in optimization processes. Here the control points are the design variables and not the key nodes. Therefore the geometry model is optimized, rather than the FE model. This leads to a smaller number of design variables while no accuracy is sacrificed. Furthermore, nodes will not be moved in a way that a different discretization stiffens the system, rather than an improved geometry.

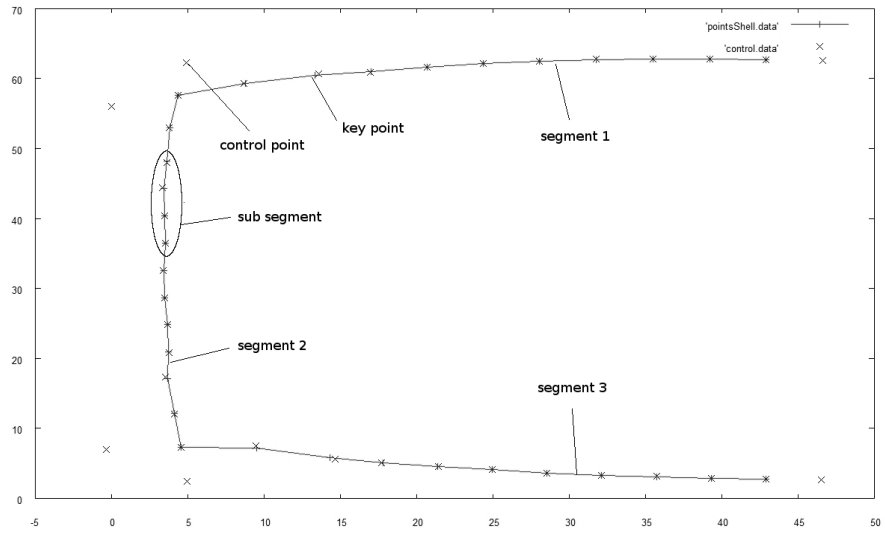

Figure 13: Key points and control points. Two key points and four control points build a sub segment. The cross section consists of three segments. Each segment is approximated by an individual B-spline.

Before the control values can be calculated the segments' end conditions have to be specified. There are two possible end conditions. The natural boundary condition, which features zero curvature at each end, is one. The advantage of that condition is that no tangent vectors have to be provided. One should be aware though, that this can cause kinks at intersections of segments. These kinks lead to the so called *C(0)* connectivity. *C(2)* connectivity, offering smooth transition from one segment to another, can be achieved by choosing the second end condition. Therefore tangent vectors have to be chosen in such a way, that they match at each intersection.

Once the control values b_i are generated, a B-spline can be evaluated at an arbitrary position. This position is governed by the parameter h. This parameter starts with *0* at one key point and ends with *1* at the following.

With the B-spline definition completed, the optimization process can be constructed. The required elements are a program that can create the control points from discrete key points and thicknesses, as well as evaluate the B-splines to obtain discrete cross sectional points and its corresponding thickness. Additionally, an FE program has to be available. In the present case this is FEAP, extended by a user developed mesh generation tool. The last part is a software that improves the design variables in order to obtain an optimum configuration of those. The sensititivities of the objective function and of the constraint, that means the pipe stiffness, required for this procedure have to be calculated as well.

The developed optimization procedure is illustrated in Figure 14 and can be described as follows: In a first step the control points of the B-splines are calculated and it is determined which are used as design variables. In case of size optimization only those control values governing the thickness variation are used. In case of shape optimization also some of those describing the x and y coordinate variation are eligible.

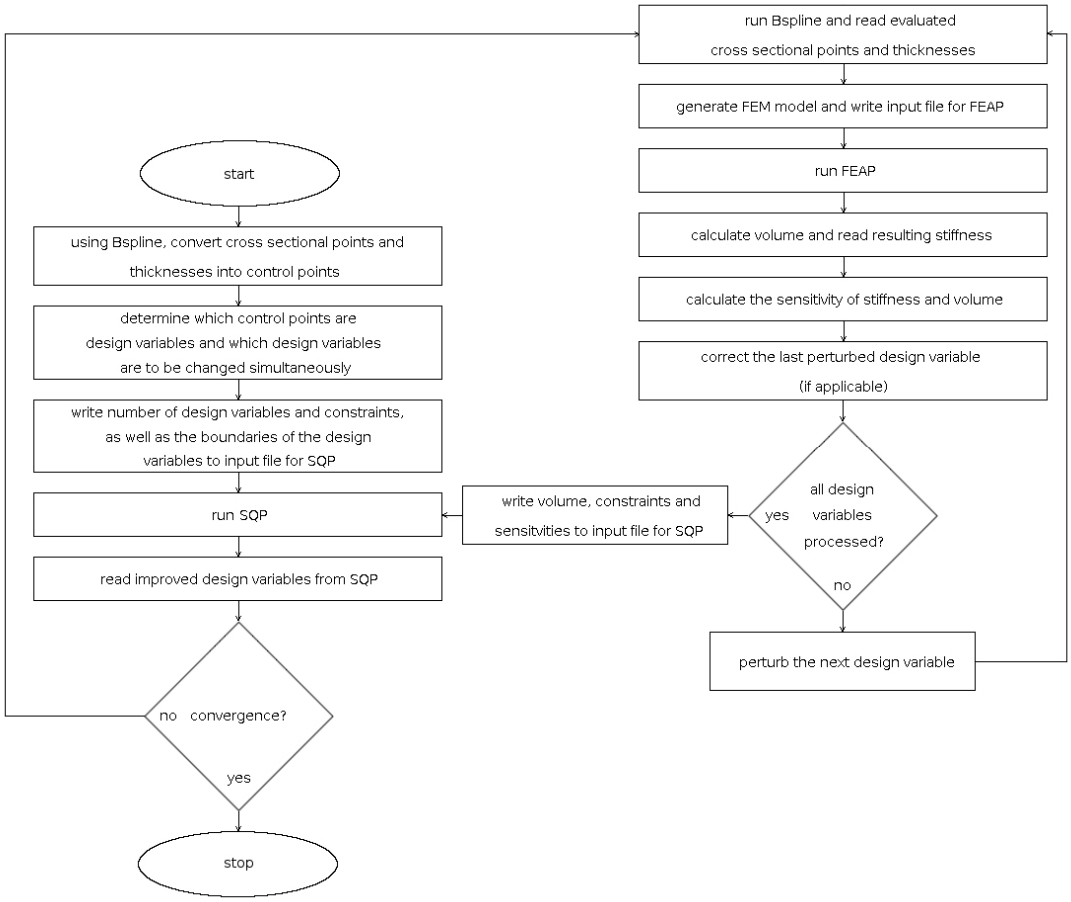

Figure 14: Flowchart of the optimization process. Three programs, B-spline, FEAP and an SQP optimizer, are coupled and can be used for size and shape optimization.

Now the optimization tool, in this case a Sequential Quadratic Programming (SQP) tool (the theoretical background can be found in [7]), is initialized with the number of design variables and the number of constraints. Furthermore, the initial design variable values and their boundaries are defined. It returns the improved design variables.

Next, the FE analysis part starts. One analysis is conducted without changing any of the design variables. All the following results within the actual iteration will be related to that initial analysis. To run that initial analysis, the design variables from the SQP are read and via the B-spline tool the geometry is generated, which is converted into the FE model. After this simulation is accomplished, the resulting pipe stiffness, as well as the pipe's volume is stored.

Subsequently n_{DV} analyses are conducted, where n_{DV} is the number of design variables. Those analyses distinguish by the design variable which is perturbed at the time. Comparing the resulting pipe stiffness and volume of the actual simulation with the initial one yields the corresponding sensitivity with respect to the active design variable. Naturally after an analysis with one perturbed design variable is finished, its pipe stiffness and volume are stored and its value is restored to the

original one. This is repeated, until all design variables are processed. The sensitivity of the objective function and the constraint with respect to the *i*-th design variable DV_i is computed according the finite difference method, shown in Equation 4.

$$\frac{df}{dDV_i} = \frac{f(DV_i) - f(DV_i + \xi \cdot DV_i)}{\xi DV_i} \tag{4}$$

Here $f(DV_i)$ is either the objective function or the constraint of the initial configuration, whereas $f(DV_i + \xi \cdot DV_i)$ is the one of a configuration where the *i*-th design variable is perturbed by a small factor ξ. This perturbation factor was found to be best as 10^{-4}.

Now the values of the objective function and the constraint as well as the corresponding sensitivities are written to a file that is read by the SQP. It then returns a set of improved design variables. The whole procedure is repeated, until convergence occurs.

The above procedure has been applied to the C-shell model with spring boundary of a 1500 mm diameter pipe. The objective was to minimize the expended material while the resulting pipe model featured a stiffness of at least 2.1 kN/m². The minimum requirement for that pipe is 2.0 kN/m², whereas experiments and simulations of the original pipe yielded an average stiffness of 3.71 kN/m². Thus the optimization improves the pipe in two ways. A profile is obtained that is less conservative, that is to say it is closer to the requirements and a wall thickness variation that provides a higher stiffness than any other.

The results have been compared to those obtained by Optistruct which has a built-in optimization tool. The design variables in either case were the thicknesses of the shell model. In the case of FEAP the control points governing the thickness distribution and in the case of Optistruct the actual shell element thicknesses.

The resulting optimum thickness variation can be seen in Figure 15.

It can be seen, that the commercial software Optistruct and the self developed tool, only consisting of open-source software, return results that are qualitatively similar. Only the thicknesses of the bottom line differ to some extent. The reason for that might be that the optimization tasks are different. In FEAP a prescribed displacement of 3 % of the internal diameter is applied. The constraint is that the vertical reaction at the bottom of the model corresponds to the desired stiffness. In Optistruct the nodes that would have this prescribed displacement are subjected to concentrated forces instead. The sum of those forces equals to the reaction demanded in FEAP. The constraint in that case is that the displacement of the nodes subjected to the forces does not exceed 3 % of the internal diameter. Two of those nodes exceed the allowed displacement by 0.2 mm, which is within the accepted violation limits of the software. Furthermore the final volume of the model in Optistruct is 569 cm^3, whereas the FEAP solution was slightly smaller with 565 cm^3. Thus the resulting thickness variation obtained with FEAP is superior to that from Optistruct.

Note that the minimum thickness was set to 3mm.

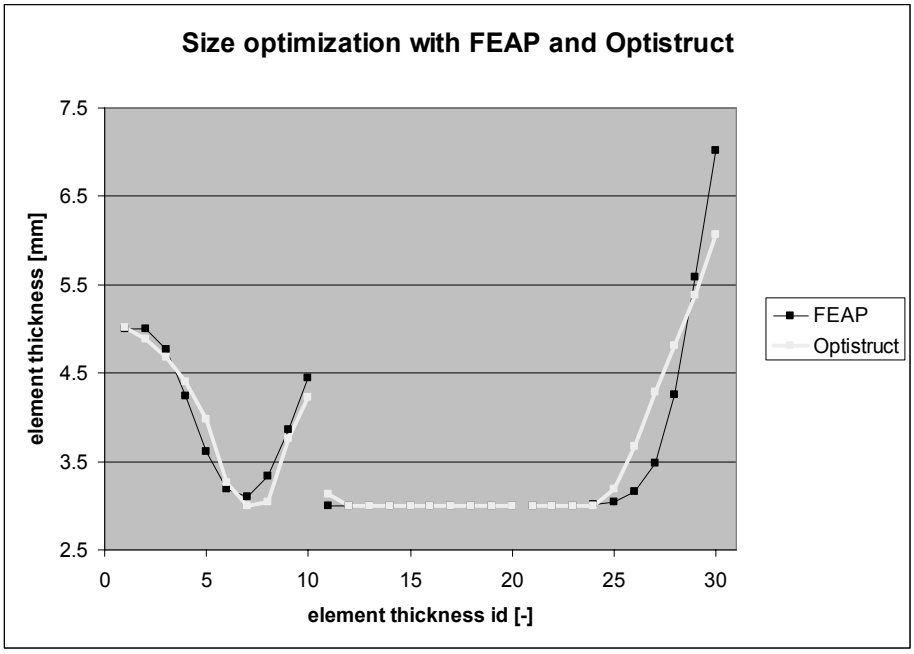

Figure 15: Optimum variation of the 30 element thicknesses, obtained by Optistruct and FEAP.

6 Results and Discussion

Extensive material tests have been conducted in order to quantify the dependence of the E-modulus upon temperature and strain rate. A representative value of 1200 MPa was used throughout all simulations and provided reasonable results. Further investigations are necessary to apprehend the influence of the strain.

Depending on the purpose of a simulation, regarding the model type, different alternatives arise from this study. For instance, if accuracy is being sought and/or the analysis of local behaviour is of interest, the model should undoubtedly be the whole profile and the mesh should contain solid elements.

If efficiency is being quested instead, there are a number of options that offer different degrees of efficiency. The C-model with springs is fast and accurate but requires the tuning of the springs' stiffness and it does not represent local behaviour. The whole model with shell elements is not as efficient as any of the C-models but it is notably more efficient than the whole model with solid elements, while it can still represent local behaviour to some extent (e.g. stresses in the corners of each box-profile cannot be analyzed accurately, but contrary to the C-models, the entire pipe is simulated, rather than an artificial substitute that merely yields the ring stiffness). Finally, the C-model with shell elements is the least accurate alternative, but the time required to obtain the ring stiffness makes it a candidate, if numerous analyses need to be carried out, for instance for optimization.

The results of the FE analyses using the whole and spring models, discretized with both, solid and shell elements, as well as available experiment data can be found in Tables 1 and 2 for the 1500 and 2100 mm pipe, respectively.

	Test 1	Test 2	Test 3	Mean
experiment	3.74	3.79	3.60	3.71
	shell		solid	
	spring	*whole*	*spring*	*whole*
Optistruct	3.57	3.55	3.72	3.63
FEAP	3.61	3.62	n.a.	n.a

Table 1: Resulting pipe stiffnesses for the 1500 diameter pipe obtained from the solid whole model compared with an average pipe stiffness of real tests.

	Test 1	Test 2	Test 3	Mean
experiment	3.10	2.62	2.68	2.80
	shell		solid	
	spring	*whole*	*spring*	*whole*
Optistruct	2.58	2.59	2.68	2.58
FEAP	2.58	2.57	n.a.	n.a

Table 2: Resulting pipe stiffnesses for the 2100 diameter pipe obtained from the solid whole model compared with an average pipe stiffness of real tests.

It should be mentioned, that the reason, why the stiffness of the solid-spring model is higher than its shell counterpart, is that the spring stiffness was tuned, utilizing the shell model and due to the significantly coarser mesh in the shell model the tuning is subjected to a certain inaccuracy. Another tuning with the solid model would naturally eliminate this discrepancy.
The resulting profile of a size optimization with FEAP and the original cross section are illustrated in Figure 16.
The objective was to minimize the volume of the pipe while its stiffness is not less than 2.1 kN/m². The design variables in FEAP were the control values of the B-spline that described the thickness variation.
Obviously, it is more efficient to concentrate the material in the middle of the two horizontal walls, while the material in the vertical wall does not contribute significantly. This improvement results in a reduction of the volume of almost 48 %, from 1084 cm^3 to 565 cm^3.
The development of the objective function during the optimization process, i.e. the volume of the model is depicted in Figure 17.

7 Conclusions

FE models with different degrees of accuracy and efficiency where sought for simulating the pipe stiffness test according to the standard BS EN 1446: 1996. This was realized, and a Java Tool and several FORTRAN 77 programs were developed, that allowed for an automated generation of those models from scanned pipe profiles, which guaranteed realistic geometry data.

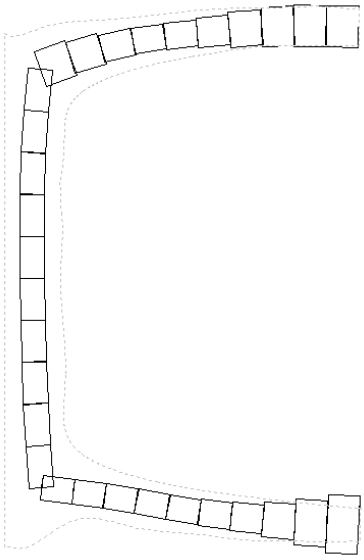

Figure 16: Original profile (dotted line) and optimized profile from FEAP.

Results from the FE analyses could be verified with real pipe stiffness tests. Given the deviation observed in those tests, the results can be called sufficiently accurate. The FE analyses were conducted with Optistruct and FEAP. Both solvers yielded almost identical solutions.
With those models at hand, an optimization tool, based on the coupling of open-source software, was developed. Its performance was successfully compared with the optimization tool built in the commercial software Optistruct. The result led to a material saving of almost 48 %.

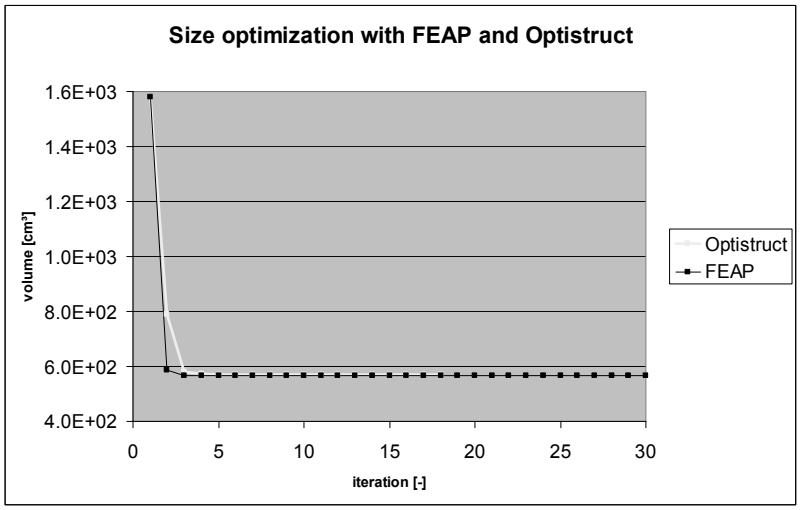

Figure 17: Development of the objective function (volume) with ongoing optimization process in Optistruct and FEAP. An optimum solution minimizes the objective function.

Acknowledgements

The first authors gratefully acknowledge the financial support from Asset International Ltd.

References

[1] British Standards Institution, "BS EN 1446 : 1996 –Plastics piping and ducting systems – Thermoplastics pipes – Determination of ring flexibility"; British Standards Institution, London, 1996.
[2] L.E. Janson, "Plastics Pipes for Water Supply and Sewage Disposal"; Borealis, Stockholm 2003
[3] Lapack, LAPACK website, http://www.netlib.org/lapack
[4] Altair Hyperworks, "Hypermesh Manual", 2006
[5] Altair Hyperworks, "Optistruct Manual", 2006
[6] Berkeley University, "FEAPpv Manual", http://www.ce.berkeley.edu/~rlt/feappv, 2005
[7] E. Hinton; J. Sienz: M. Özakça, "Analysis and Optimization of Prismatic and Axisymmetric Shell Structures"; Springer-Verlag, London, 2003